J Mol Model (2010) 16:129–136
DOI 10.1007/s00894-009-0526-x

ORIGINAL PAPER

Design and synthesis of thiourea based receptor containing naphthalene as oxalate selective sensor

Nongnit Morakot · Wandee Rakrai · Somchai Keawwangchai · Chatthai Kaewtong · Banchob Wanno

Received: 2 February 2009 / Accepted: 21 April 2009 / Published online: 13 June 2009

Abstract The thiourea based receptor containing naphthalene groups (**1**), has been successfully designed and synthesized for application as an oxalate receptor. A density functional theory at B3LYP/6-31G(d,p) level of theory has been applied to predict the binding ability between **1** and selected anions, *i.e.*, oxalate, malonate, succinate, glutarate, dihydrogen phosphate, and hydrogen sulphate. Calculation results point out that receptor **1** shows the strongest interaction to oxalate ion with the binding free energy of 172.48 kcal mol^{-1}. The recognition ability of **1** to the selected anions has been also investigated by means of the absorption and emission techniques. Experimental results are in excellent agreement with the calculation data in which receptor **1** shows highly selective for oxalate ion over the other anions with logβ of 3.82 (0.02) M^{-1} by means of the size of binding cavity.

Keywords Anion receptor · DFT · Naphthalene · Oxalate · Thiourea

Introduction

The design and synthesis of anion receptors have been interesting for many years, especially, in the field of supramolecular chemistry [1–6]. Sensitive and selective sensors for anions are the major need of the designing. Moreover in the designed process, the receptor for recognition of anions is also based on synthetic feasibility. One successful approach for preparing anion receptors is addition of hydrogen bond donors to an organic skeleton to yield receptors that can interact with anions through hydrogen bonding.

Hosts containing a variety of donor groups have been investigated. Examples include thioureas, ureas, amines, amides, thioamides, sulfonamides, indole, and pyrroles [4–10]. Thiourea based receptors have been used more extensively for anion detection [4, 5]. A variety of receptors containing one or more thiourea subunits have been designed and tested for anion recognition and sensing over the past years [6]. Moreover, the selectivity is also related to the energy of the receptor-anion interaction. Whereas strong hydrogen bond interactions are established with anions containing the most electronegative atoms. Theoretical study to gain more properties, *i.e.*, geometrical structure, binding energy, molecular orbital, and charge transfer, on the origin of molecular recognition affinity has largely been known to be a potential tool. A number of reports on the theoretical prediction of selectivity trends of anions with specific receptor units have been found in the last decade [11–14]. However, the preferential interaction of oxyanions with thiourea based receptor has received a few theoretical attentions [15, 16].

In the present work, theoretical calculation under the density functional theory (DFT) method has been used to design and complexation study the thiourea based receptor containing naphthalene with anions. Then synthesis and complexation ability of designed receptor with anions have been experimentally studied.

Computational details

Structures of thiourea based-receptor **1**, and its complexes with oxoanion acceptors oxalate, malonate, succinate,

N. Morakot · W. Rakrai · S. Keawwangchai · C. Kaewtong · B. Wanno (✉)
Department of Chemistry, Faculty of Science,
Mahasarakham University,
Mahasarakham 44150, Thailand
e-mail: banchobw@gmail.com

glutarate, hydrogen sulphate, and dihydrogen phosphate have been optimized by using the DFT method. The DFT calculation has been performed using the Becke's three-parameter exchange functional with the Lee-Yang-Parr correlation functional (B3LYP) [17]. All calculations have been performed using the MO computations at the B3LYP/6-31G(d,p) level of theory [18]. Stationary points have been fully optimized without any constrains and characterized by vibrational frequency calculations, which also provided zero point vibrational energies (ZPE). The vibrational frequency computations have been carried out at 298.15 K and standard pressure [19]. The highest occupied molecular orbital (HOMO), the lowest unoccupied molecular orbital (LUMO), and the energy gap ($\Delta E_{\text{HOMO-LUMO}}$) have also been investigated at the same level of theory. Thermodynamic property changes of complexation are defined as the difference between thermodynamic properties of the receptor/anion complex and summation of thermodynamic properties of its fragments.

In addition, natural bond orbital (NBO) analysis implemented in GAUSSIAN 03 program [20] was applied through a series of intermolecular interactions under the above system to evaluate the NBO charges. The MOLDEN 4.2 program [21] was utilized to display the molecular structure, monitor the geometrical parameters and observe the molecular geometry convergence *via* the Gaussian output file. The molecular graphics of all related species were generated with the MOLEKEL 4.3 program [22].

Experimental section

Reagents

Solvents were purified and stored under nitrogen atmosphere. Dimethyl sulfoxide (DMSO) was dried with calcium hydride and distilled in reduced pressure. All anions were used in the form of tetrabutylammonium (TBA) salts purchased from Fluka. All reagents were standard analytical grade purchased from Merck and were used without further purification. Commercial grade solvents such as acetone, hexane, dichloromethane, methanol, and ethyl acetate were distilled before use.

General methods

^{1}H and ^{13}C NMR spectra were recorded on a Varian 400 MHz spectrometer in deuterated chloroform. MALDI-TOF mass spectra were recorded on a Biflex Bruker Mass spectrometer using 2-cyano-4-hydroxycinnamic acid (CCA) or 2,5-dihydroxy-benzoic acid (DHB) as a matrix. All UV-vis experiments were carried out on Perkin Elmer Lambda 25 UV-vis spectrometer at 298 K. Fluorescence spectra were recorded on Perkin Elmer LS50B Luminescence spectrometer. Column chromatography was carried out using silica gel (Kieselgel 60, 0.063 – 0.200 mm, Merck).

Synthesis of thiourea based receptor **1**

Thiourea based receptor **1** was prepared by using reaction of 2-(2-(2-aminoethoxy) ethoxy)ethanamine and isothiocyanatonaphthalene in the chloroform ($CHCl_3$) solution and stirred under inert atmosphere at room temperature for 12 hr (as demonstrated in Scheme 1) then the white precipitate was obtained and filtrated. The precipitate was dissolved in CH_2Cl_2 and extracted with distilled water and diluted HCl solution, respectively. The crude product was separated by column chromatography (60:40 ethyl acetate: hexane) and recrystallized in methanol. The receptor **1** was obtained as a pure yellow solid in 77% yield. The receptor **1** was characterized and confirmed by ^{1}H NMR, ^{13}C NMR, and mass spectral analysis.

Characteristics of thiourea based-receptor **1** obtained under ^{1}H NMR, ^{13}C NMR and MS techniques are listed in the following data: ^{1}H NMR (400 MHz, $CDCl_3$) δ 8.09 (s, 2H, ArN*H*C(=S)NH), δ 7.94 (br m, 2 H, Ar*H*), δ 7.85 (br m, 4 H, Ar*H*), δ 7.44 (t, J = 7.60, 2 H, Ar*H*), δ 7.37 (d, J = 7.20, 2 H, Ar*H*), δ 7.26 (s, 2 H, ArNHC(=S)N*H*), δ 3.59 (br s, 4 H, NHCH_2CH$_2$O), δ 3.28 (s, 4 H, NHCH$_2$CH_2O), δ 3.03 (s, 4 H, OCH_2CH_2O); ^{13}C NMR (400 MHz, $CDCl_3$) δ 181.46, 134.62, 131.70, 129.88,

Scheme 1 The proposed reaction of receptor **1** synthesis

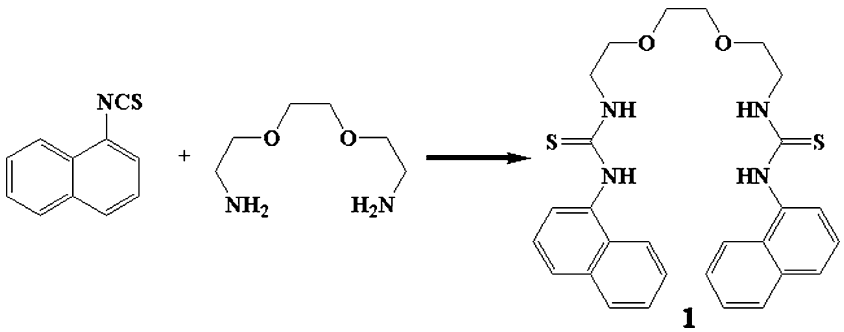

128.93, 128.50, 127.33, 127.02, 125.73, 125.17, 122.49, 69.80, 69.11, 44.89; MS (MALDI-TOF) Calcd for $[C_{28}H_{30}N_4O_2S_2]^+$: *m/z* 518.18. found: *m/z* 536.72 [M + $H_2O]^+$.

UV-vis complexation study

The complexation abilities of receptor **1** with various anions (oxalate, malonate, succinate, glutarate, hydrogen sulphate and dihydrogen phosphate) were first investigated by using UV-vis spectrometric titration in DMSO at 25°C. When necessary, 0.01 M Bu_4NPF_6 was employed to keep the ionic strength. Then 2 mL of 5.5×10^{-5} M receptor solution was placed in a spectrometric cell of 1 cm path length. The spectrum was recorded from 250 to 500 nm. The solution of anion was added into the cell from a microburette. The mixture was stirred for 40 s and spectral variation was recorded in each addition. Then the stability constant was calculated from spectrometric data using the SIRKO program [23].

Fluorescence complexation study

All fluorescence spectra were recorded in DMSO by adding 0.01 M Bu_4NPF_6 as supporting electrolyte at 25°C. The stock solutions (1.0×10^{-3} M) of the TBA salts were prepared in DMSO. Stock solution of receptor **1** (1.0×10^{-3} M) was also prepared in DMSO. For all measurements of fluorescence spectra, excitation was at 300 nm with excitation and emission slit widths at 5.0 and 5.0 nm, respectively. The fluorescence excess experiments were performed using 5.5×10^{-5} M of **1** in DMSO solution with 2.2×10^{-3} M of the TBA salts.

Results and discussion

Geometrical structures and energies

Geometrical structures of the receptor **1** and its anion complexes have been computed by full geometrical optimization without any constrains. Figure 1 displays the B3LYP/6-31G(d,p)-optimized geometries of receptor which has two stable isomers, *cis*-like (**1**) and *trans*-like (**1′**) forms. The isomer **1** is more stable than isomer **1′** by about 10.20 kcal mol^{-1}. Molecular symmetry of **1** and **1′** is found to be C_1 symmetry. Optimized geometries of anion complexes of **1** with oxoanion acceptors (oxalate, malonate, succinate, glutarate, hydrogen sulphate, and dihydrogen phosphate) are displayed in Fig. 2 which demonstrates the interesting binding features. As shown in Fig. 2, it is clearly seen that the molecular geometry of **1** found in all complexes distorts from its free form and a large number

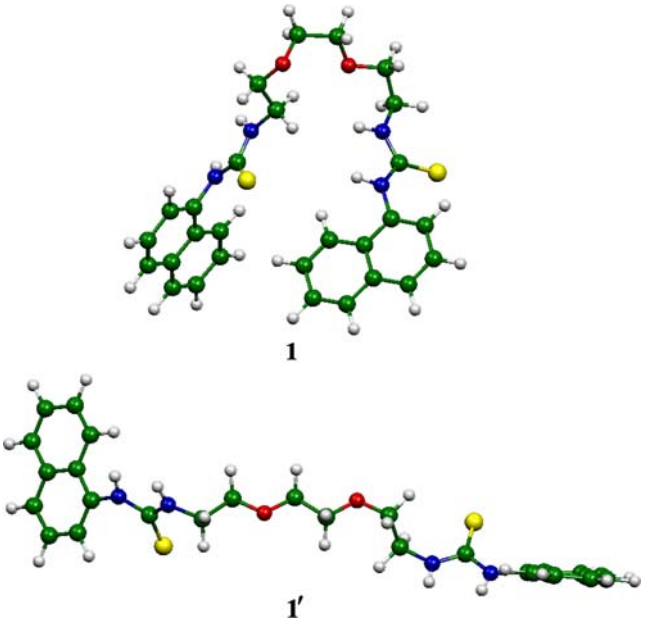

Fig. 1 The B3LYP/6-31G(d,p)-optimized structures of isomers **1** and **1′**

of intermolecular hydrogen bonds (NH···O) appeared in all complexes. The NH···O hydrogen bond distances are ranged from 1.652 to 1.986 Å. Six hydrogen bonds are found in dicarboxylate complexes (**1**/oxalate, **1**/malonate, **1**/succinate and **1**/glutarate) while for dihydrogen phosphate and hydrogen sulphate, only four hydrogen bonds are found.

The zero-point vibrational correction binding energies (ΔE_{ZPE}) in gas phase of complexation between **1** and various anions obtained from B3LYP/6-31G(d,p) calculation are tabulated in Table 1. Thermodynamic property changes, *i.e.*, enthalpy (ΔH), entropy (ΔS) and Gibbs free energy (ΔG) changes are also tabulated in Table 1. As a consideration of binding energy, enthalpy and Gibbs free energy changes of complexations, the negative value of changes indicates that all of complexations are thermodynamically stable. Whereas the **1**/oxalate complex forms the most stable complex with the ΔE_{ZPE} and ΔG of -181.70 and -172.48 kcal mol^{-1}, respectively. Interestingly, the complexation ability is strongly depending on both intermolecular hydrogen bond distances and number of hydrogen bonds. Based on the binding free energy, relative stabilities of oxoanion complexes are found to be in decreasing order: **1**/oxalate > **1**/malonate > **1**/succinate > **1**/glutarate > **1**/dihydrogen phosphate > **1**/hydrogen sulphate.

Frontier molecular orbital energies and NBO charges

The E_{LUMO} and E_{HOMO} energies, frontier molecular orbital energy gaps ($\Delta E_{HOMO\text{-}LUMO}$), chemical hardness, electron-

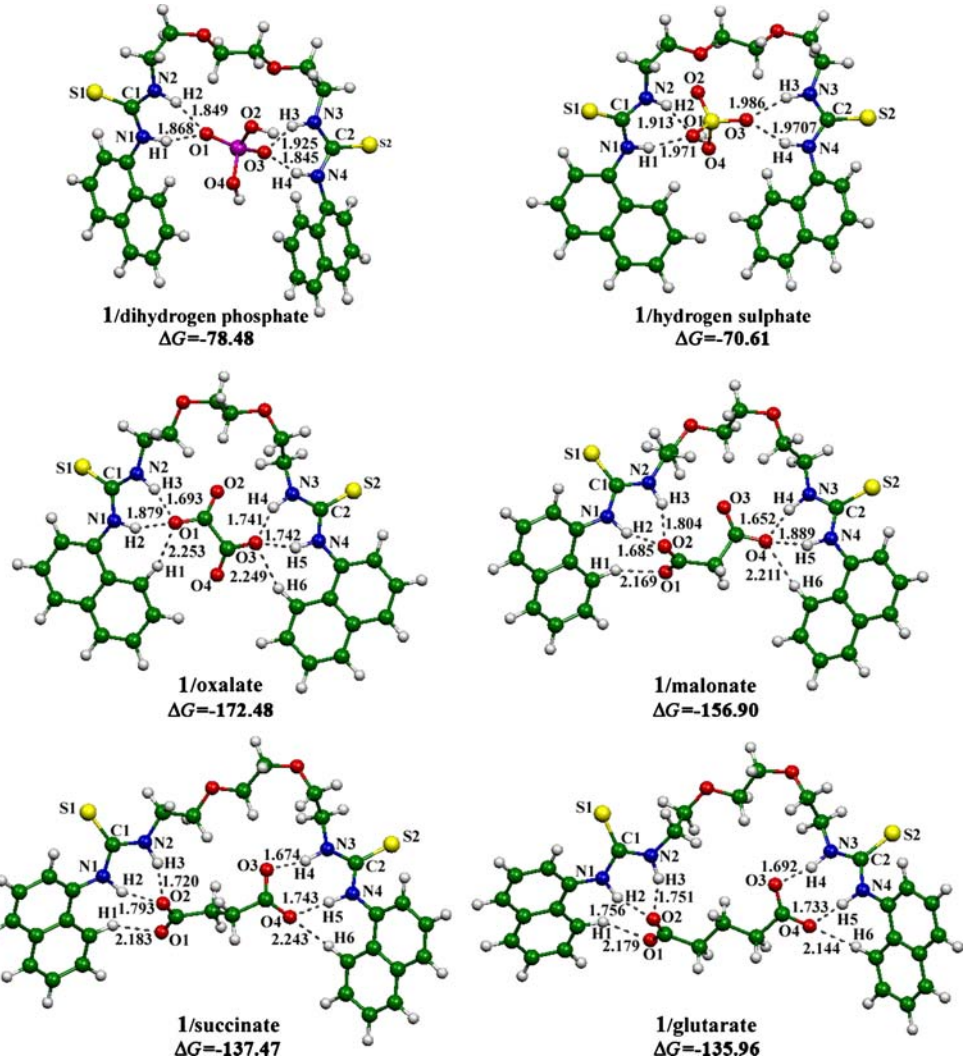

Fig. 2 The B3LYP/6-31G(d,p)-optimized structures of **1**/hydrogen sulphate **1**/dihydrogen phosphate, **1**/oxalate, **1**/malonate, **1**/succinate and **1**/glutarate. The presented hydrogen bond distances and binding free energies are in angstrom and kcal mol^{-1}, respectively

ic chemical potential and electronegativity of receptor **1** and its anion complexes computed at the B3LYP/6-31G(d,p) level are presented in Table 2. The result shows that the $\Delta E_{\text{HOMO-LUMO}}$ found in all anion complexes is slightly different and within the range of 3.34 to 3.95 eV. In addition, the high value of $\Delta E_{\text{HOMO-LUMO}}$ found in all complexes support the stable complexes formed in complexation. [24] These results are in good agreement with binding energy data which are in negative value.

Table 1 Thermodynamic properties of receptor **1** complex with various anions obtained at the B3LYP/6-31G(d,p) level of theory

Receptor/acceptor	ΔE_{ZPE} [a,b]	ΔH [a]	ΔG [a]	ΔS [c]
1/oxalate	−181.70	−179.02	−172.48	246
1/malonate	−166.22	−163.57	−156.90	255
1/succinate	−148.95	−147.33	−137.47	258
1/glutarate	−145.73	−143.47	−135.96	270
1/hydrogen sulphate	−80.67	−80.14	−70.61	238
1/dihydrogen phosphate	−90.67	−89.93	−78.48	237

[a] In kcal mol^{-1}

[b] Total energy with zero-point energy corrections

[c] In cal mol^{-1} K^{-1}

The HOMO and LUMO orbitals of receptor **1**, **1**/oxalate and **1**/dihydrogen phosphate complexes presented over isosurface value of 0.05 a.u. are displayed in Fig. 3. It is found that most of HOMO and LUMO orbitals of **1** and **1**/dihydrogen phosphate locate on the same area which is on naphthyl groups and sulfur atoms of receptor **1**. For the strongest interaction complexes (**1**/oxalate), the HOMO orbital locates on oxalate ion while the LUMO orbital locates on naphthyl group of receptor **1**. Table 3 displays the selected NBO atomic charges (in Debye) for the optimized structures of free anions, **1** and their anion complexes. From calculated NBO charge results, the charge transfers between anions and receptor are investigated and implied the presence of receptor - anion interaction. The highest in charge transfer is found in **1**/oxalate complex with the value of 0.955 electrons.

Table 2 HOMO, LUMO, and $\Delta E_{\text{HOMO-LUMO}}$ of receptor **1** and its oxoanion complexes computed at the B3LYP/6-31G(d,p) level of theory

Receptor/acceptor	E_{HOMO} [a]	E_{LUMO} [a]	$\Delta E_{\text{HOMO-LUMO}}$ [a]	η [a, b]	μ [a, c]	χ [a, c]
1	−5.069	−1.402	3.667	1.834	−3.236	3.236
1/oxalate	−0.030	3.449	3.479	1.740	1.710	1.710
1/malonate	−0.332	3.011	3.343	1.672	1.340	1.340
1/succinate	−0.627	3.056	3.684	1.842	1.215	1.215
1/glutarate	−0.740	2.995	3.733	1.867	1.128	1.128
1/hydrogen sulphate	−2.843	1.108	3.951	1.976	−0.868	0.868
1/dihydrogen phosphate	−2.777	1.007	3.786	1.893	−0.885	0.885

[a] In eV unit

[b] Chemical hardness, $\eta = \Delta E_{\text{HOMO-LUMO}}/2$

[c] Electronic chemical potential, $\mu = (E_{\text{HOMO}} + E_{\text{LUMO}})/2$

[d] Mulliken electronegativity, $\chi = -(E_{\text{HOMO}} + E_{\text{LUMO}})/2$.

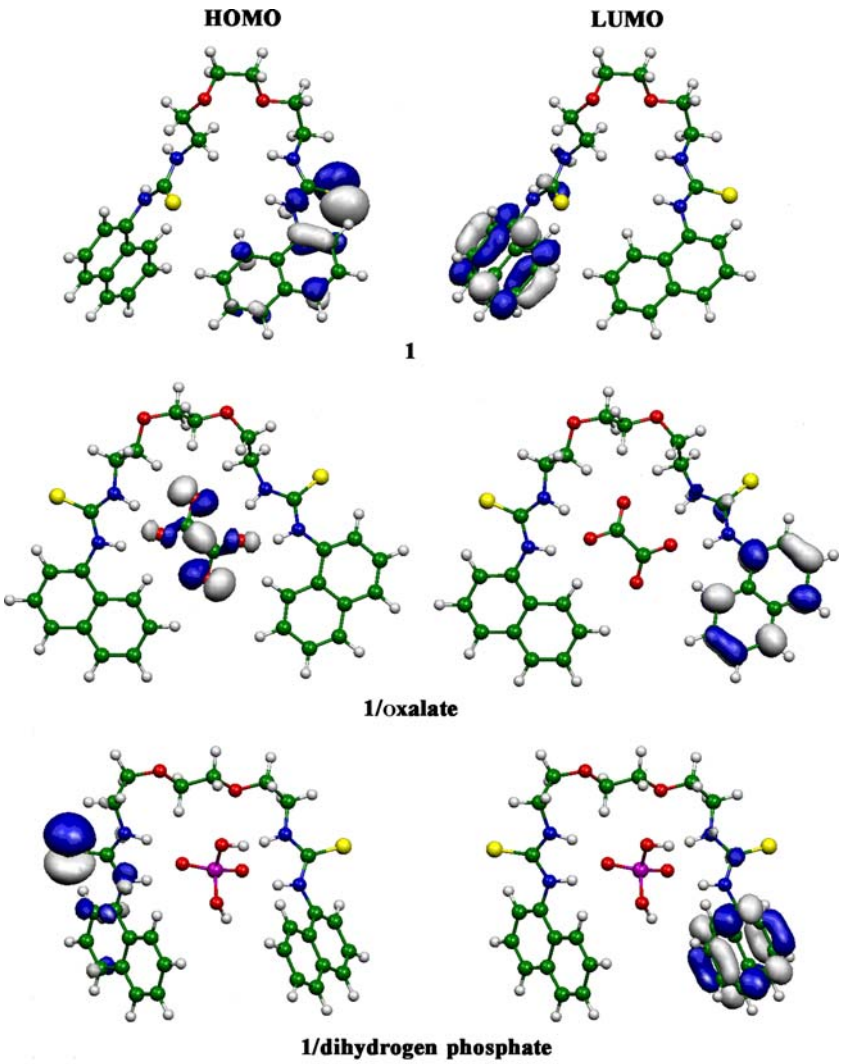

Fig. 3 The B3LYP/6-31G(d,p)-computed molecular orbitals contoured, HOMOs (Left) and LUMOs (Right) at an iso-surface value of 0.05 a.u. for free receptor **1**, **1**/oxalate and **1**/dihydrogen phosphate

Table 3 The selected NBO atomic charges (in Debye) for the optimized structures of free anions, **1** and complexes computed at the B3LYP/6-31G(d,p) level of theory

Atoms [a]	Receptor or complexes						
	1	**1**/oxalate	**1**/malonate	**1**/succinate	**1**/glutarate	**1**/hydrogen sulphate	**1**/dihydrogen phosphate
S1	−0.260	−0.385	−0.379	−0.381	−0.379	−0.327	−0.341
S2	−0.263	−0.395	−0.401	−0.404	−0.395	−0.330	−0.337
C1	0.271	0.302	0.301	0.305	0.301	0.290	0.293
C2	0.273	0.306	0.306	0.307	0.303	0.292	0.292
C3	-	0.731	0.847	0.823	0.824	-	-
C4	-	0.730	0.819	0.829	0.829	-	-
N1	−0.628	−0.618	−0.624	−0.632	−0.634	−0.623	−0.630
N2	−0.633	−0.630	−0.628	−0.631	−0.633	−0.639	−0.641
N3	−0.636	−0.624	−0.623	−0.634	−0.631	−0.628	−0.631
H1	0.415	0.460	0.459	0.463	0.464	0.453	0.460
H2	0.410	0.452	0.458	0.457	0.463	0.451	0.459
H3	0.418	0.467	0.468	0.454	0.455	0.448	0.459
H4	0.419	0.463	0.464	0.460	0.461	0.451	0.460
O1	-	−0.793	−0.833	−0.727	−0.728	−1.041	−1.165
O2	-	−0.763	−0.745	−0.832	−0.828	−0.991	−1.026
O3	-	−0.812	−0.814	−0.784	−0.758	−1.020	−1.181
O4	-	−0.725	−0.730	−0.772	−0.792	−0.943	−1.041

[a] Atomic labels are tabulated in Fig. 2.

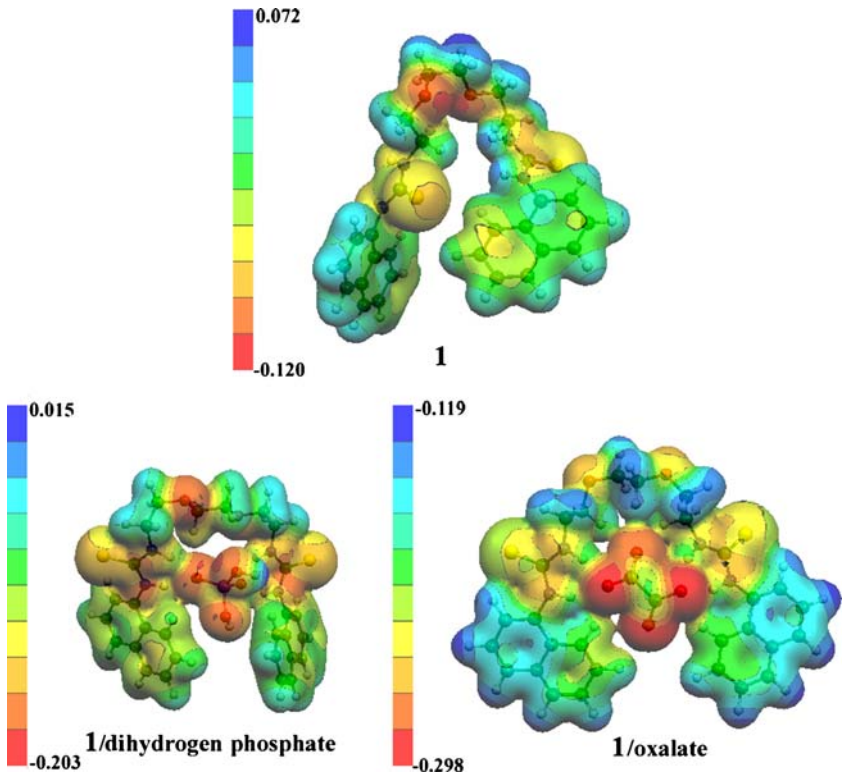

Fig. 4 The electrostatic potentials (in a.u.) of **1**, **1**/oxalate and **1**/dihydrogen phosphate obtained at B3LYP/6-31G(d,p) level and presented over electronic isodensity $\rho = 0.05$ eÅ^{-3}. (For interpretation of the references to color in this figure legend, the reader is referred to the web version of this article.)

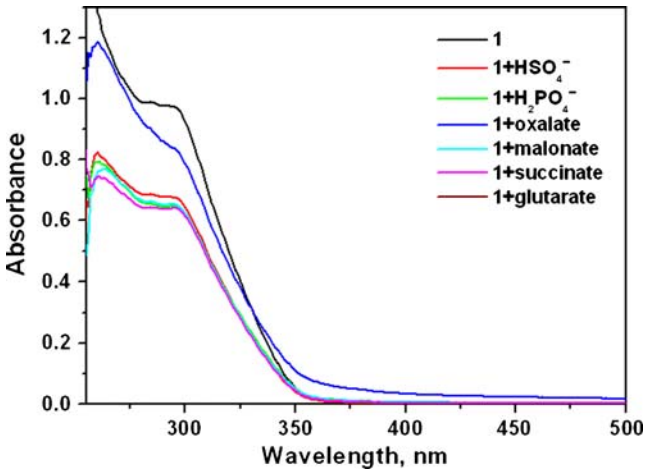

Fig. 5 UV-vis spectra changes of receptor **1** upon addition of various anions. Conditions: **1** (5.5×10^{-5} M) in DMSO, TBA salts (30 equiv) in DMSO

Electronic potential surface

Electrostatic potential surfaces of receptor **1**, **1**/oxalate and **1**/dihydrogen phosphate complexes have been generated from the GAUSSIAN output files of the B3LYP/6-31G (d,p) computation with GFPRINT and POP = FULL keywords, using the Molekel 4.3 software [22]. The electrostatic potentials (in a.u.) presented over electronic isodensity $\rho = 0.05$ eÅ^{-3} are illustrated in Fig. 4. From the graphical map of electronic isodensity surface of receptor **1**, it shows strong positive charge on both thiourea protons (H_N) with intent blue. After complexation with anions, thiourea protons of **1** are reduced in their intent blue or positive charge which confirmed the electron transfer process. Moreover, Fig. 4 also displays that oxalate ion can induce receptor **1** to form the strongly "fitting" structure with lock and key behavior as found in the previous report of the thiourea and/or thioamide based receptors for anion recognition [4–6]. For further understanding in anion binding property of the designed receptor **1**, complexation ability of **1** was studied and discussed in the next section.

Complexation of thiourea based receptor 1

The complexation ability of the receptor **1** to oxoanions was investigated by monitoring the changes in the absorption and emission spectra of the solution of **1** upon addition of various anions. Absorbance spectrum of **1** (Fig. 5) measured in DMSO shows a broad band below 350 nm. When a high excess of anions in the form of tetrabutylammonium salts was added, the absorption spectrum of **1** is significantly decreased in its intensity. Most of the anions added in **1** solution can decrease intensity of **1** spectrum to nearly the same level. Surprisingly, only addition of oxalate ion decreases the intensity of receptor **1** spectrum to the different level compared to other anions and a shoulder on the red-side of the absorption appears. The crossing of spectra between **1** and its complex with oxalate ion to form an isobestic point at 330 nm clearly shows the present of only two light-absorbing species (the free host and the host-guest complex) in solution. This result demonstrates that complexation occurs *via* hydrogen bonding to stabilize the electronic excitation state of the chromophore [25]. In addition, UV-vis spectroscopy was also employed to determine the stability constant for the complexation between **1** and oxalate ion by using the SIRKO program [23]. Figure 6 displays the absorption spectral change of **1** in DMSO upon addition of oxalate ion. Increasing the oxalate concentration produces the decreas-

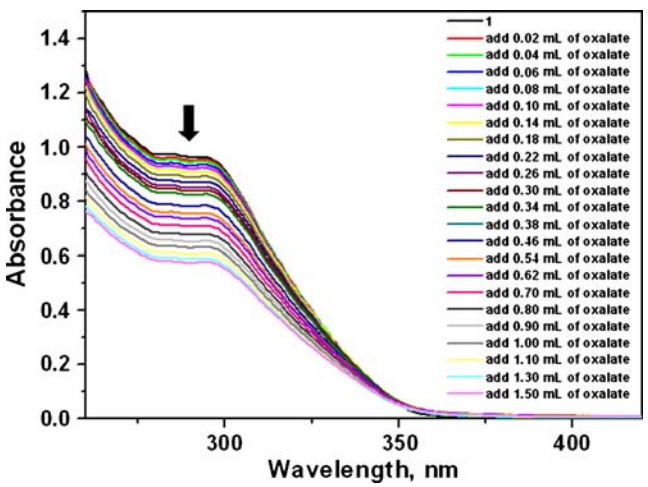

Fig. 6 Spectral change in the UV-vis absorption of receptor **1** ($C_L = 5.5 \times 10^{-5}$ M) upon addition of oxalate ion ($C_A = 2.2 \times 10^{-3}$ M) in DMSO ($0 \le C_A/C_L \le 30$)

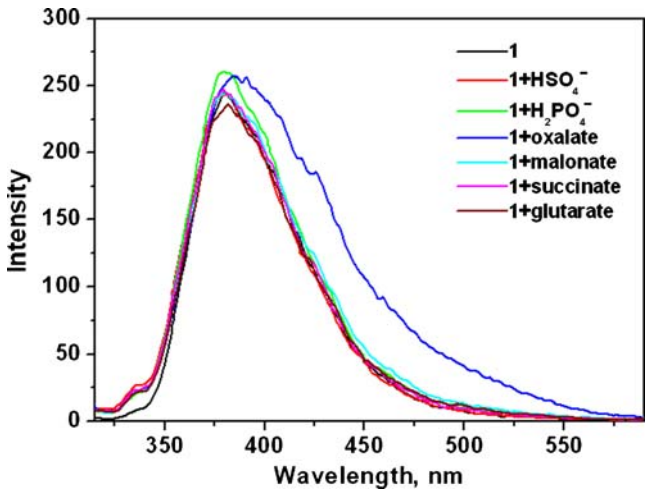

Fig. 7 Fluorescence changes of receptor **1** upon addition of various anions. Conditions: **1** (5.5×10^{-5} M) in DMSO, excitation at 300 nm, TBA salts (30 equiv) in DMSO

ing of absorption intensity of **1**. According to the extent of the absorption spectral change, the association constant of **1** is obtained and shows that receptor **1** binds strongly to oxalate ion with 1:1 (**1**:oxalate) stoichiometric complex (logβ of 3.82 (0.02) M^{-1}).

Figure 7 displays the emission spectral change of **1** upon addition of various anions. Receptor **1** (5.5×10^{-5} M in DMSO) on excitation at 300 nm exhibits an emission band at 380 nm. The addition of malonate, succinate, glutarate, dihydrogen phosphate and hydrogen sulphate anions (30 equiv) to a solution of **1** is the reason for the slight change in its fluorescent spectra. Interestingly, upon addition of oxalate ion, the fluorescent spectrum of **1** is shifted from 380 to 390 nm and increased its intensity too. These results indicate that the fluorescent change is caused by photoinduced charge transfer (PCT) process between the receptor and naphthyl moiety [26–28]. These interactions are in agreement with stabilization of the intramolecular charge transfer excited state responsible for red-shifted absorption band. The difference in absorption and emission behaviors of **1**/oxalate comparing to other anion complexes of **1** shows that receptor **1** is higher selective to oxalate ion than that of other anions.

Conclusions

The thiourea based receptor containing naphthalene (**1**) has been successfully designed and synthesized for application as an oxalate sensor. A density functional theory at B3LYP/6-31G(d,p) level of theory has been applied to predict the binding ability of receptor **1** with oxoanions oxalate, malonate, succinate, glutarate, dihydrogen phosphate, and hydrogen sulphate. It is found that receptor **1** shows the strongest interaction to bind with oxalate ion with the binding free energy of 172.48 kcal mol^{-1}. The trend of binding ability is in decreasing order: oxalate > malonate > succinate > glutarate > dihydrogen phosphate > hydrogen sulphate. Furthermore, the electronic properties, especially the highest occupied molecular orbital (HOMO) and lowest unoccupied molecular orbital (LUMO) of receptor **1** and its complexes with anions, have also been reported. The result shows that the HOMO and LUMO energy gaps are slightly different. The recognition ability of the receptor **1** has been also investigated by monitoring the changes in the absorption and emission spectra of the solution of **1** upon addition of various anions. Experimental results are in excellent agreement with the calculation data in which receptor **1** shows the highest selectivity for oxalate ion over the other anions with logβ of 3.82 (0.02) M^{-1}.

Acknowledgments The authors would like to appreciate the Faculty of Science, Mahasarakham University and the Postgraduate Education and Research in Chemistry (PERCH) program, for financial support. The facilities provided by Supramolecular Chemistry Research Unit, Faculty of Science, Mahasarakham University and Department of Chemistry, Faculty of Science, Chulalongkorn University, Thailand are also gratefully acknowledged.

References

1. Schmidtchen FP, Berger M (1997) Chem Rev 97:1609–1646
2. Kaewtong C, Fuangswasdi S, Muangsin N et al. (2006) Org Lett 8 (8):1561–1564
3. Beer PD, Gale PA (2001) Angew Chem Int Ed Engl 40:486–516
4. Sessler JL, Sansom PI, Andriersky A et al. (1997) In: Bianchi A, Bowman-James K, García-España E (eds) Supramolecular Chemistry of Anions. Wiley, New York
5. Lehn JM (1995) Supramolecular chemistry, Concepts and Perspectives. VCH, Weinheim, Germany
6. Suksai C, Tuntulani T (2003) Chem Soc Rev 32:192–202
7. Gale PA (2003) Coord Chem Rev 240:191–221
8. Kim SK, Yoon J (2002) Chem Commun 770–771
9. Cho EJ, Ryu BJ, Lee YJ et al. (2005) Org Lett 13:2607–2609
10. Brooks SJ, Gale PA, Light ME (2006) Chem Commun 4344–4346
11. Navakhuna K, Ruangpornvisuti V (2007) THEOCHEM 806(1–3):145–153
12. Ruangpornvisuti V, Wanno B (2007) J Mol Model 13(1):65–77
13. Ruangpornvisuti V (2004) THEOCHEM 686(1–3):47–55
14. Suvire FD, Cabedo N, Chagraoui A et al. (2003) THEOCHEM 666–667:455–467
15. Jose DA, Singh A, Das A, Ganguly B (2007) Tetrahedron Lett 48:3695–3698
16. Wanno B, Rakrai W, Keawwangchai S, Morakot N, Morakot N, Nunthaboot N, Ruangpornvisuti V (2009) THEOCHEM 902:33–40
17. Becke AD (1988) Phys Rev A 38(6):3098–3100
18. Lee C, Yang W, Parr RG (1988) Phys Rev B 37:785–789
19. Ochterski JW (2000) Thermochemistry in Gaussian. Gaussian Inc, Pittsburgh, PA
20. Frisch MJ, Trucks GW, Schlegel HB et al. (2008) Gaussian 03, Revision E.01. Gaussian Inc, Wallingford, CT
21. Schaftenaar G (1991) MOLDEN 4.2. CAOS/CAMM Center Nijmegen. Toernooiveld, Nijmegen, Netherlands
22. Flükiger P, Lüthi HP, Portmann S et al. (2000) MOLEKEL 4.3. Swiss center for scientific computing. Manno, Switzerland
23. Vetrogon VI, Lukyanenko NG, Schwing-well MJ et al. (1994) Talanta 41:2105–2112
24. Pearson RG (1997) Chemical hardness: Application from molecules to solids. Wiley, New York
25. Nishizawa S, Kato R, Hayashita T et al. (1998) Anal Sci 14 (3):595–597
26. Valeur B, Leray I (2000) Coord Chem Rev 205:3–40
27. Kim SK, Bok JH, Bartsch RA et al. (2005) Org Lett 7:4839–4842
28. Kim HJ, Kim SK, Lee JY et al. (2006) Org Chem 71:6611